Polymer 51 (2010) 164–177

Contents lists available at ScienceDirect

Polymer

journal homepage: www.elsevier.com/locate/polymer

Poly(ε-caprolactone) acrylates synthesized using a facile method for fabricating networks to achieve controllable physicochemical properties and tunable cell responses

Lei Cai, Shanfeng Wang*

Department of Materials Science and Engineering, The University of Tennessee, Knoxville, TN 37996, USA

ARTICLE INFO

Article history:
Received 28 October 2009
Received in revised form
15 November 2009
Accepted 21 November 2009
Available online 26 November 2009

Keywords:
Poly(ε-caprolactone) acrylate (PCLA)
Photo-crosslinking
Cell responses

ABSTRACT

We present a facile method to synthesize photo-crosslinkable poly(ϵ-caprolactone) acrylates (PCLAs) and reveal tunable cell responses to photo-crosslinked PCLAs. Including three PCL diacrylates (PCLDAs) and two triacrylates (PCLTAs), PCLAs could be fabricated into polymer networks with controllable physical properties to satisfy diverse tissue-engineering needs, for example, bone and nerve regeneration. This novel synthetic method used potassium carbonate (K_2CO_3) as the proton scavenger other than widely used triethylamine (TEA) in order to avoid colorization and potential toxicity from the side reaction between TEA and acryloyl chloride. In addition, this new method significantly simplified the purification step of the polymer products because of the convenient separation between inorganic particles and organic polymer solution. Through combining crystallite-based physical network and crosslink-based chemical network together, we could modulate material properties and consequently control cell responses. Thermal properties such as glass transition temperature (T_g), melting temperature (T_m), and crystallinity (χ_c) of both uncrosslinked and crosslinked PCLAs were correlated with their mechanical and rheological properties. Surface characteristics such as surface morphology, hydrophilicity, and its capability of adsorbing serum proteins from cell culture medium were also examined for crosslinked PCLA disks. Mouse MC3T3 cells and rat Schwann precursor cell line (SPL201) cells were applied to evaluate the *in vitro* biocompatibility of these polymeric networks and the roles of surface chemistry, crystallinity, and stiffness in regulating cell attachment, spreading and proliferation collectively. Semi-crystalline PCLA network with the highest χ_c and T_m was found to support cell attachment, spreading, and proliferation best among all these five systems.

1. Introduction

In the past several decades, polymeric biomaterials have been attracting much attention as they can satisfy different clinical needs such as replacement of diseased tissues [1,2]. We aim to develop novel injectable or crosslinkable polymeric biomaterials with suitable physicochemical properties for bone and nerve regeneration. For bone regeneration, these crosslinkable polymers can be injected and hardened *in situ* to fill bone defects that result from the resection of primary and metastatic tumors or skeletal trauma [3,4]. Three-dimensional (3D) pre-formed devices such as bone scaffolds and nerve conduits can also be fabricated using these crosslinkable polymers [5–7]. Polymer nerve conduits are used to bridge the gap between injured peripheral nerve stumps, aiming to replace the present gold standard autologous nerve grafts, which have numerous disadvantages such as limited source, additional surgery, loss of nerve function in transplantation, and mismatch between injured nerve and donor nerve [8–12].

Material hardening or gelation can be induced by thermal or photo-crosslinking or physical associations [13]. In this study, we combined crystallite-connected physical network with chemical network formed by photo-crosslinking process, which is more efficient and faster than thermal crosslinking [14–27]. Among many photo-crosslinkable polymeric biomaterials [14–27], several systems have been developed through the condensation between α,ω-dihydroxy poly(ε-caprolactone) (PCL diol), an oligomeric end-functionalized form of FDA-approved biomaterial PCL for applications such as controlled drug delivery and suture [28], and unsaturated anhydrides/acid chlorides such as maleic anhydride, itaconic anhydride [17], acryloyl chloride [19,20], methacryloyl chloride [21], and fumaryl chloride [7,22–26] or crosslinkable macromers such as poly(propylene fumarate) (PPF) [27]. Specifically, PCL diacrylates

* Corresponding author. Tel.: +1 865 974 7809; fax: +1 865 974 4115.
E-mail address: swang16@utk.edu (S. Wang).

0032-3861/$ – see front matter © 2009 Elsevier Ltd. All rights reserved.
doi:10.1016/j.polymer.2009.11.042

(PCLDAs) were synthesized between PCL diol and acryloyl chloride in benzene using triethylamine (TEA) as the proton scavenger [19]. Recently we found that acryloyl chloride or fumaryl chloride formed a colored complex with TEA in the reaction and consequently polymers synthesized using this method can be colorized, encumbering their photo-crosslinking and cell staining in later use [29]. In addition, such colored complexes demonstrated cytotoxicity at a low concentration of 0.01 g/L in cell culture medium [29].

To solve this colorization problem, previously we have applied potassium carbonate (K_2CO_3) as a substitute of TEA in synthesizing uncolorized photo-crosslinkable PCL fumarates (PCLFs) [23]. PCLFs have been used to fabricate nerve conduits for guiding axon growth in peripheral nerve regeneration [7] and prepare composites with hydroxyapatite nanoparticles for bone-tissue-engineering applications [26]. In this study, we extended this facile method to synthesize crosslinkable PCL acrylates (PCLAs) including both PCLDAs and PCL triacrylates (PCLTAs) from three PCL diols and two PCL triols with different molecular weights. We further characterized their chemical structures and physical properties. Compared with PCLFs having fumarate segments to connect an unknown number of PCL blocks [7,22–26], PCLAs possessed more reactive acrylate segments on the chain ends with a theoretical number of 2 or 3. Therefore, PCLAs were expected to crosslink more efficiently to form networks with better-defined crosslinking density and distance between two neighboring crosslinks. As the molecular weight of PCL precursor increased within the range studied here, the crystallinity and melting point of both PCLA and PCLA network formed increased significantly. Thus a wide range of material properties could be achieved using this series of PCLAs.

The purposes of this study is not only to supply a facile synthetic method of photo-crosslinkable polymers and a library of their controllable physical properties for satisfying diverse tissue-engineering needs, but also to examine the material design strategy of combining crystallite-based physical network and crosslink-based chemical network together for modulating both material properties and cell responses. Polymer disks, tubes, and porous scaffolds have been fabricated via photo-crosslinking to demonstrate the feasibility of manufacturing medical devices using this series of PCLAs. Thermal properties such as glass transition temperature (T_g), melting temperature (T_m), and crystallinity (χ_c) have been examined and correlated with their mechanical and rheological properties.

The correlation between material properties and cell/tissue–material interactions is the central task for tissue-engineering and clinical considerations [30–32]. Surface chemical, morphological, and mechanical properties are major factors in determining cell–material interactions [30–32]. Particularly, extensive investigations have been performed on revealing the role of surface stiffness using synthetic hydrogels coated with adhesive proteins [33–35]. Crosslinked PCLFs were used previously to demonstrate the role of crystallinity in regulating mechanical properties and then responses of rat bone marrow stromal cells (BMSCs) and Schwann precursor cell line (SPL201) cells [7,26]. With well-controlled architecture, crystallinity, mechanical properties, and surface characteristics, crosslinked PCLAs in the present study are better model polymers than crosslinked PCLFs to investigate the roles of various surface physicochemical factors in regulating attachment, spreading, and proliferation of mouse MC3T3-E1 and rat SPL201 cells. Surface characteristics including surface morphology, hydrophilicity, and its capability of adsorbing serum proteins from cell culture medium are considered. The significance of this study lies in offering solid evidence that PCL crystalline structures play a critical role in enhancing both mechanical properties and cell attachment and proliferation, which is important for understanding cell–material interactions and selecting appropriate materials for biomedical applications.

2. Materials and methods

2.1. Synthesis of poly(ϵ-caprolactone acrylate)s (PCLAs)

PCL diols with nominal molecular weights of 530, 1250, and 2000 g mol^{-1} and PCL triols with nominal molecular weights of 300 and 900 g mol^{-1} were purchased from Aldrich (Milwaukee, WI) and had chemical structures of H–[O(CH_2)$_5$CO–]$_m$OCH_2CH_2–O–CH_2CH_2O[–OC(CH_2)$_5$O]$_n$–H and C_2H_5C[CH_2O[CO(CH_2)$_5$O]$_n$H]$_3$ (Fig. 1), respectively. Prior to acrylation, PCL precursors were dried overnight in a vacuum oven at 50 °C. All other chemicals were also purchased from Aldrich unless otherwise noted. Methylene chloride was dried and distilled over calcium hydride (CaH_2) before the reaction. Acryloyl chloride was used as received. Ground K_2CO_3 was dried at 100 °C overnight and then cooled down in vacuum.

As described in Fig. 1, acryloyl chloride, PCL diol or triol, and K_2CO_3 were measured out in a molar ratio of 3:1:3. PCL diol or triol was dissolved in methylene chloride (1:2 v/v) and placed in a 250 mL three-neck flask along with K_2CO_3 powder. The mixture was stirred with a magnetic stirrer to form a slurry, to which acryloyl chloride dissolved in methylene chloride (1:10 v/v) was added dropwise. The reaction mixture was maintained at room temperature under nitrogen for 24 h. After reaction, the mixture was filtered to remove the solids (KCl, $KHCO_3$, and unreacted K_2CO_3). The filtrate was then added dropwise to diethyl ether and the precipitate was rotary-evaporated to yield an oil-like or wax-like product, depending on the molecular weight.

2.2. Characterizations of PCLAs

Gel permeation chromatography (GPC) was carried out at room temperature using an integrated GPC system (PL-GPC 20, Polymer Laboratories, Inc.) with a refractive index detector to determine the molecular weights and polydispersity of PCL precursors and PCLAs. The data were processed using Cirrus GPC/SEC software (Polymer Laboratories). Tetrahydrofuran (THF) was used as the eluent at a flow rate of 1.0 mL/min and standard monodisperse polystyrenes (Polymer Laboratories) were used for calibration. Fourier Transform Infrared (FTIR) spectra were obtained on a Perkin Elmer Spectrum Spotlight 300 spectrometer with Diamond Attenuated Total Reflectance (ATR). ^{1}H Nuclear Magnetic Resonance (NMR) spectra were acquired on a Varian Mercury 300 spectrometer using $CDCl_3$ solutions containing tetramethylsilane (TMS). Elemental microanalysis of PCLTAs synthesized in the presence of TEA or K_2CO_3 was performed in Complete Analysis Laboratories, Inc (Parsippany, NJ).

Differential Scanning Calorimetry (DSC) measurements were performed on a Perkin Elmer Diamond differential scanning calorimeter in a nitrogen atmosphere. To keep the same thermal history, samples were first heated from room temperature to 100 °C and cooled to −90 °C at a cooling rate of 5 °C/min. Then a subsequent heating run was performed from −90 °C to 100 °C at a heating rate of 10 °C/min. Wide-angle X-ray diffraction (WAXD) patterns were obtained in reflection using an X'pert X-ray diffractometer and CuKα radiation. Thermogravimetric Analysis (TGA) was performed on a TA Q50 thermal analyst in flowing nitrogen at a heating rate of 20 °C/min. Zero-shear viscosities (η_0) of uncrosslinked PCLAs were measured from the Newtonian region at various temperatures up to 120 °C using a strain-controlled rheometer (RDS-2, Rheometric Scientific) in the frequency (ω) range of 0.1–100 rad/s. A 25 mm diameter parallel plate flow cell and a gap of ~0.5 mm were used.

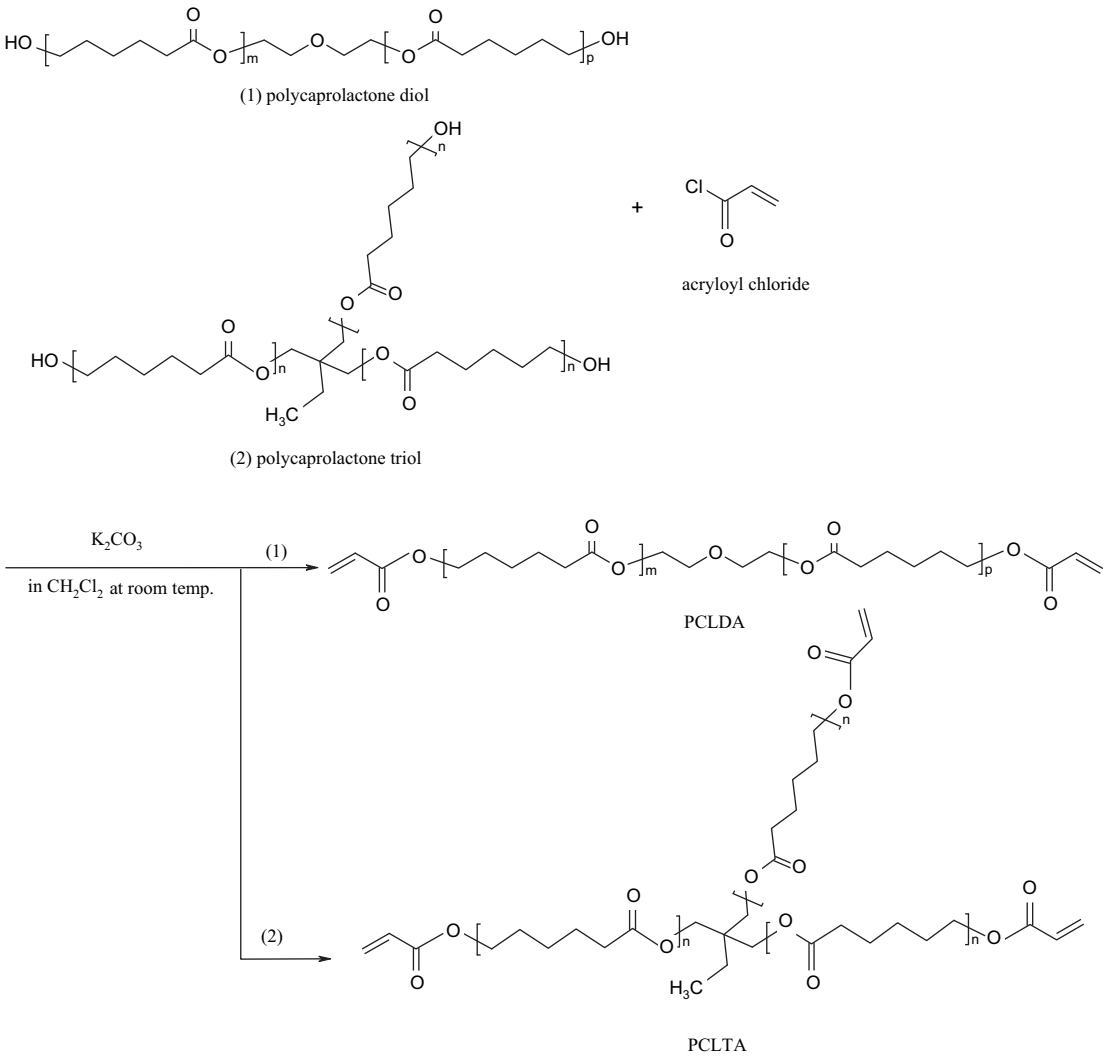

Fig. 1. Synthesis of PCLAs.

2.3. Photo-crosslinking of PCLAs

Photo-crosslinking was initiated with ultraviolet (UV) light ($\lambda = 315$–380 nm) from a Spectroline high-intensity long-wave UV lamp (SB-100P, Intensity: 4800 uw/cm^2) in the presence of photo-initiator phenyl bis(2,4,6-trimethyl benzoyl) phosphine oxide (BAPO, IRGACURE 819™, Ciba Specialty Chemicals, Tarrytown, NY). In crosslinking, 75 μL of BAPO/CH_2Cl_2 (300 mg/1.5 mL) solution were mixed with pre-dissolved PCLA/CH_2Cl_2 solution (1.5 g/500 μL). However, no pre-dissolved solution was needed for PCLDA530 and PCLTA300. Homogeneous PCLA/BAPO/CH_2Cl_2 mixture was transferred into a mold consisting of two glass plates (2.1 mm, thickness) and a Teflon spacer (0.37 mm, thickness). The filled mold was placed under UV light with a distance of ~7 cm from the lamp head for 20 min. Crosslinked PCLA sheets were removed from the mold after cooled down to room temperature. Strips and disks with different dimensions were cut from the sheets for various experimental purposes. In fabricating porous bone scaffolds, PCLDA2000/BAPO/CH_2Cl_2 solution was mixed with salt (sodium chloride) particles (300–400 μm, size). The mixture was crosslinked under UV light for 30 min. Porous scaffolds (5 mm × 3 mm, length × diameter) with a porosity of 80% were obtained after the salt particles were leached away in water. For fabricating nerve conduits, homogenous PCLA2000/BAPO/CH_2Cl_2 mixture mentioned earlier was injected from a syringe to a custom mold formed using a glass tube, a stainless steel wire, and two plastic end-caps. The mold loaded with viscous polymer solution was rotated under the UV light for 20 min to facilitate crosslinking. As other specimens, crosslinked PCLDA2000 nerve conduits were soaked in acetone for two days to remove the residue of BAPO and sol fraction before dried in vacuum.

2.4. Characterizations of crosslinked PCLAs

For determining the gel fractions and swelling ratios of crosslinked PCLAs, two crosslinked PCLA disks (8 mm × 1.0 mm, diameter × thickness) for each solvent were immersed in excess CH_2Cl_2 and water. After two days, polymer disks were taken out and weighed after blotted quickly. The solvent in the disks was subsequently evacuated and the dry disks were weighed. Based on the measured weights of the original (W_0), dry (W_d, CH_2Cl_2 was the solvent for determining gel fractions), and fully swollen (W_s) PCLA disks, their swelling ratios and gel fractions were calculated using the equations of $(W_s - W_d)/W_d \times 100\%$ and $W_d/W_0 \times 100\%$, respectively.

Linear viscoelastic properties of crosslinked PCLAs, including storage modulus (or shear modulus) G' and loss modulus G'' as well as viscosity η as functions of frequency, were measured using the same rheometer (see Section 2.2) at 20, 37, and 60 °C, sequentially. Rheological measurements were performed with

a small strain ($\gamma = 1\%$) using an 8 mm diameter parallel plate flow cell and a gap of ~0.5 mm, depending on the thickness of polymer disk. Torsional modulus was measured on crosslinked PCLA strips (~40 mm × ~8 mm × ~1.5 mm, length × width × thickness) with a strain of 1% in the frequency range of 0.1–100 rad/s at 37 °C using the rheometer.

Tensile and compressive properties of crosslinked polymer specimens were implemented using a dynamic mechanical analyzer (DMTA-5, Rheometric Scientific) at both room temperature and 37 °C. Briefly, polymer strips (~30 mm × ~1.5 mm × ~0.3 mm, length × width × thickness) were pulled and polymer disks (~2.5 mm × ~1.0 mm, diameter × thickness) were compressed at a strain rate of 0.001 s^{-1}. At least five specimens for each sample were measured and averaged.

Surface morphology of crosslinked PCLDA disks was characterized using a multimode atomic force microscopy (AFM) with a Nanoscope V control system (Veeco Instruments, Santa Barbara, CA). Tapping-mode images were acquired at room temperature with a scan size of 20 μm × 20 μm at a scan rate of 0.5 Hz. Topography of the surfaces was recorded simultaneously with a standard silicon tapping tip on a beam cantilever and the root mean square (RMS) roughness was calculated from height images. Crosslinked PCLDA disk surfaces and cross-sections of a conduit and a porous scaffold made from crosslinked PCLDA2000 were examined using scanning electron microscopy (SEM) (S-3500, Hitachi Instruments Inc., Tokyo, Japan).

2.5. Contact angle measurement and protein adsorption

A Ramé-Hart NRC C. A. goniometer (Model 100-00-230, Mountain Lakes, NJ) was used to measure the contact angle of water on crosslinked PCLA disks. Approximately 1 μL of distilled water (pH = 7.0) was injected onto the disk surface and the measurement was performed after a static time of 30 s. A tangent method was used to calculate the contact angle in degrees. For each sample, three disks were used and six data points were taken for calculating average and standard deviation.

As described previously [24], in protein adsorption measurement, pre-wetted crosslinked PCLA disks (8 mm × 0.8 mm, diameter × thickness) were immersed in MC3T3 cell culture medium (see Section 2.6) for 4 h at 37 °C. Then the disks were transferred into 48-well plates (one disk per well) and 600 μL of phosphate buffer saline (PBS) was used to wash the disks three times. Five minutes of gentle agitation was applied and PBS was discarded after each wash. Two hundred forty microliters (240 μL) of 1% sodium dodecyl sulfate (SDS) solution was put into these wells for 1 h at room temperature. The SDS solution was collected in a plastic vial and new SDS solution was put into the wells for another 1 h. This procedure was repeated twice and all the SDS solution was collected in a plastic vial. The concentrations of protein in the collected SDS solutions were determined on a micro-plate reader (SpectraMax Plus 384, Molecular Devices, Sunnyvale, CA) using a MicroBCA protein assay kit (Pierce, Rockford, IL). Albumin in the kit was used to prepare solutions in SDS with eight known concentrations in order to construct a standard curve.

2.6. Cell culture and in vitro cytocompatibility

Mouse MC3T3-E1 pre-osteoblast cells (CRL-2593, ATCC, Manassas, VA) and rat SPL201 cells were used to evaluate the cytocompatibility of crosslinked PCLAs for potential applications in bone and nerve regeneration, respectively. Newly purchased MC3T3-E1 cells were cultured *in vitro* using Alpha Minimum Essential Medium (Gibco, Grand Island, NY), supplemented with 10% fetal bovine serum (FBS) (Sera-Tech, Germany) and 1% penicillin/streptomycin (Gibco). Cryo-preserved SPL201 cells were thawed and plated on polystyrene flasks in culture medium that contained Dulbecco's modified eagle medium (Gibco), 10% FBS, 1% penicillin/streptomycin, and 10 ng/ml human recombinant EGF (Pepro Tech Inc., Rocky Hill, NJ). After plating, cell suspension was incubated for 12 h in a 5% CO_2, 95% relative humidity incubator at 37 °C. Cell culture medium was changed after 24 h of plating the cells. Cells were split when they were 80% confluent. Trypsin with a concentration of 0.025% was used to bring the cells off from the flasks. The passage number of SPL201 cells was between 8 and 20.

Cytotoxicity evaluation proceeded by harvesting MC3T3 and SPL201 cells from the flasks and seeding them in 24-well plates at a density of 2×10^4 cells/cm^2 with 500 μL/cm^2 of primary medium. After purification in acetone and drying, crosslinked PCLA disks were sterilized in excess 70% ethanol solution overnight with gentle shaking. Then the disks were dried again in vacuum and washed with PBS at least three times prior to use. Through culture medium, cells were exposed to the sterile polymer disks (8 mm × 0.8 mm, diameter × thickness) inside trans-wells for 1, 4, and 7 days for SPL201 cells and 1, 2, and 4 days for MC3T3 cells, respectively. Wells seeded with cells at the same density while no exposure to polymer disks were positive controls and empty wells were negative controls. UV absorbance at 490 nm was determined on the incubated MTS assay solution (CellTiter 96 Aqueous One Solution, Promega, Madison, WI) using the same micro-plate reader as described in Section 2.5 and cell viability was expressed by the normalization of UV absorbance to the positive controls' average value.

2.7. In vitro cell attachment and proliferation

MC3T3 and SPL201 cell attachment and proliferation were performed to demonstrate the effect of material properties on cell responses. Sterile crosslinked PCLA disks were placed on the bottom of 48-well tissue-culture plates using autoclave-sterilized inert silicon-based high-temperature vacuum grease (Dow Corning, Midland, MI) to avoid floating in the culture medium. Cells were seeded onto the polymer disks at a density of 2×10^4 cells/cm^2. Culture medium was removed from the wells and the polymer disks were washed with PBS twice after cells were cultured in a humidified atmosphere of 5% CO_2 at 37 °C for 4 h, 1, 2, 4 days for MC3T3 cells and 4 h, 1, 4, and 7 days for SPL201 cells. Attached cells were fixed in 16% paraformaldehyde (PFA) solution for 10 min. After PFA solution was removed, the cells were washed twice with PBS and permeabilised with 0.2% Triton X-100. Then the cells were stained using rhodamine-phalloidin for 1 h at 37 °C and DAPI at room temperature for photographing using an Axiovert 25 light microscope (Carl Zeiss, Germany). Cell area was determined and averaged on 20 non-overlapping cells at 4 h post-seeding using ImageJ software (National Institutes of Health, Bethesda, MD).

2.8. Statistical analysis

Student's *t*-test was performed to assess the statistical significance ($p < 0.05$) of the differences between results.

3. Results and discussion

3.1. Structural characterizations

In the discussion below, PCL precursors and PCLAs are named with the nominal molecular weights of PCL precursors (Table 1). PCLAs synthesized in the presence of K_2CO_3 were white when they were semi-crystalline or colorless when amorphous. The content of nitrogen was measured to be 0.86 wt% and 2.35 wt% for PCLTA300 and 900 synthesized using TEA as the proton scavenger,

Table 1
Molecular characteristics and thermal properties of the polymers in this study.

Polymer	M_n (g mol^{-1})	M_w (g mol^{-1})	DPI	Thermal properties				
				T_g (°C)	T_m (°C)	ΔH_m (J/g)	X_c (%)	T_d (°C)
PCL diol530	1080	1180	1.1	–	5.5	25.3	19.3	258
PCL diol1250	2470	3330	1.4	–	44.8	61.0	45.8	374
PCL diol2000	3470	5200	1.5	−68.6	49.7	68.3	51.1	378
PCL triol300	670	670	1.0	−65.5	–	–	–	223
PCL triol900	1380	1720	1.2	−67.8	26.4	34.3	26.4	326
PCLDA530	1120	1390	1.2	–	22.9	44.8	36.8	393
PCLDA1250	2990	4150	1.4	–	46.1	68.7	52.9	405
PCLDA2000	3510	5150	1.5	−57.9	49.1	74.4	56.9	406
PCLTA300	720	740	1.0	−70.5	–	–	–	368
PCLTA900	2030	2440	1.2	−70.6	28.9	55.7	45.0	405
Crosslinked PCLDA530	–	–	–	−58.3	–	–	–	407
Crosslinked PCLDA1250	–	–	–	−58.0	34.8	39.6	30.4	412
Crosslinked PCLDA2000	–	–	–	−57.1	39.2	44.5	34.1	414
Crosslinked PCLTA300	–	–	–	−52.5	–	–	–	402
Crosslinked PCLTA900	–	–	–	−53.6	–	–	–	404

respectively. In contrast, nitrogen was not detectable (<0.02 wt%) in PCLTAs synthesized using K_2CO_3. The use of K_2CO_3 also simplified synthesis and purification greatly because inorganic particles could be separated easily from the polymer solution through centrifugation or filtration. In addition, methylene chloride was used to replace the more toxic solvent, benzene, used in the previous method [19]. Recently, this method has been also applied successfully in our laboratory to synthesize photo-crosslinkable polyethylene glycol (PEG) acrylates and poly(L-lactide) (PLLA) acrylates to avoid colorization or contamination from the yellow complex formed between acryloyl chloride and TEA.

GPC results of all PCLAs synthesized in this study as well as their PCL precursors are listed in Table 1. It should be noted that the molecular weights and physical properties of these PCL diol or triol precursors purchased vary from lot to lot although their nominal molecular weights are labeled identical. For example, PCL530 used in our previous studies had a T_m at 26.2 °C and was wax-like at room temperature [22,23,27]. While the T_m was as low as 5.5 °C for the present PCL530 and it was a translucent viscous fluid instead. The weight-average molecular weights (M_ws) of all PCLAs were higher than those of their PCL diol or triol precursors as the result of acrylation.

The chemical structures of PCLAs were confirmed using FTIR and ^{1}H NMR spectra in Figs. 2 and 3, respectively. In the FTIR spectra of PCL precursors, PCLAs, and crosslinked PCLAs, the absorption peaks at 1635 cm^{-1} in PCLAs could be assigned to the vinyl (H_2C=CH–) groups from the acrylation of PCL diols and triols. The disappearance of this peak after photo-crosslinking suggested that the carbon–carbon double bond was consumed to form polymer networks. The absorption bands at 2950 and 1740 cm^{-1} in all the samples were attributed to methylene (–CH_2–) and ester carbonyl (–C=O) groups, respectively. The absorption peak around 3500 cm^{-1} for hydroxyl (-OH) groups in PCL diols and triols became weaker in both uncrosslinked and crosslinked PCLAs as they were replaced by acylate groups and later crosslinked. In the ^{1}H NMR spectra shown in Fig. 3, all the chemical shifts could be well assigned to the corresponding protons in the polymer structures demonstrated below the spectra. Evidently PCLAs demonstrated vinyl groups (-CH=CH-) in the chemical shift δ range of 5.7–6.5 ppm, in agreement with literature [19,20].

3.2. Photo-crosslinking and characteristics of crosslinked PCLAs

Before crosslinking, PCLDA530, PCLTA300 and 900 were viscous fluids while PCLDA1250 and 2000 were wax-like at room temperature, none of which had sufficient mechanical properties for load-bearing applications. Zero-shear viscosities (η_0) of these PCLDAs at different temperatures above their T_m were plotted against temperature in Fig. 4. The viscosities of PCLDA530 and PCLTA300 at room temperature were sufficiently low to be fabricated into scaffolds directly using stereolithographic methods without being diluted in an organic solvent [6], which generates inconvenience and safety concerns in processing and brings toxicity in applications if not removed. Arrhenius equation $\eta(T) \sim \exp(E_a/RT)$ [36] was applied to interpret the temperature dependence of viscosity for all these polymers. R is the universal gas constant (8.314 J K^{-1} mol^{-1}), T is the absolute measurement temperature (K), and E_a is the activation energy in the above equation [36]. The activation energy E_a obtained by plotting log η_0 against $1/T$ (Fig. S1) was 11.8, 24.1, 24.7, 20.7, and 34.4 kJ/mol for PCLDA530, 1250, 2000, PCLTA300 and 900, respectively. These values showed a trend of approaching to 40 kJ/mol for PCL samples with much higher molecular weights [37].

Gel fraction indicates the efficiency of crosslinking in polymer chains and decides the integrity of crosslinked products. Photo-crosslinking for 5, 10, 15, 20, and 30 min was performed on PCLDA530. The gel fraction of crosslinked PCLDA530 increased with crosslinking time from 0.762 to 0.832, 0.854, 0.881, and 0.882, respectively. Therefore, 20 min was chosen to photo-crosslink all

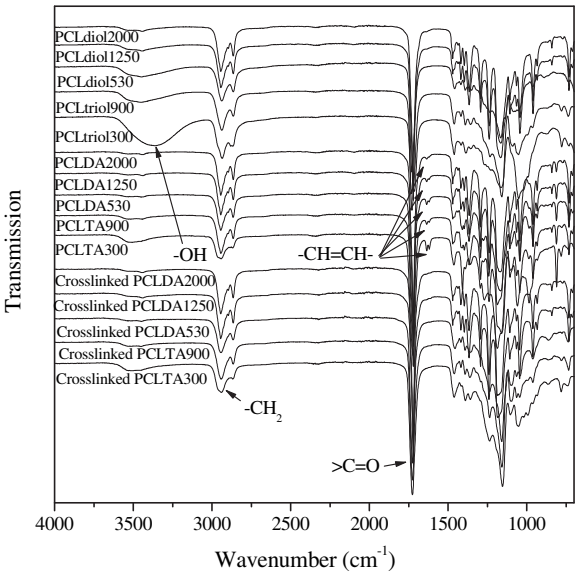

Fig. 2. FTIR spectra of PCL precursors, PCLAs, and crosslinked PCLAs.

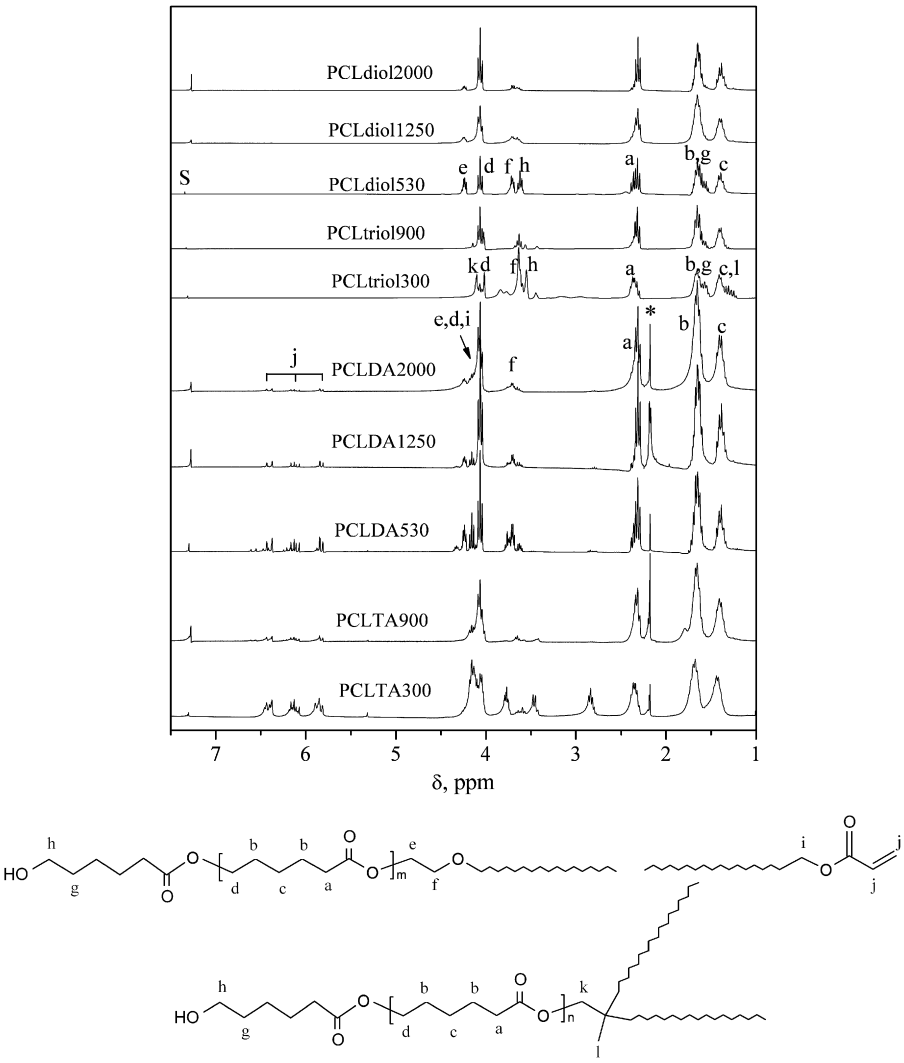

Fig. 3. ^{1}H NMR (300 MHz, $CDCl_3$, reference TMS) spectra of PCL precursors and PCLAs. S = solvent. Asterisk denotes the signals due to the residue of acetone.

PCLAs because it was sufficient for achieving high gel fractions without causing over-cure problems such as warping and cracks in crosslinked products. Unlike PCLFs with multiple fumarate segments along one polymer chain [7,22–26], the maximum number of acrylate segments could only be 2 for PCLDAs or 3 for PCLTAs. As the result, there was no evident dependence of photo-initiator BAPO for the gel fraction and mechanical properties of the polymer networks when BAPO amount was varied in crosslinking. In contrast, BAPO amount can be used to modulate PCLF networks' gel fraction, thermal and mechanical properties [25].

The gel fraction of crosslinked PCLDA530, 1250, 2000, PCLTA300 and 900 was 0.88 ± 0.01, 0.82 ± 0.02, 0.69 ± 0.01, 0.91 ± 0.03, and 0.85 ± 0.002, respectively. These values were higher than those of their PCLF counterparts photo-crosslinked at the same condition [7,22–26] because the double bonds in acrylates without steric hindrance were more reactive than those in fumarates. In addition, PCLTAs had three active acrylate end groups for crosslinking. The swelling ratio of crosslinked PCLA in methylene chloride increased from 2.2 for crosslinked PCLDA530 to 5.6 for crosslinked PCLDA1250 and 10.6 for crosslinked PCLDA2000 as the distance between two neighboring crosslinks in the network increased. Because of the same reason, the swelling ratio for crosslinked PCLTA300 was 2.5 while it increased to 5.1 for crosslinked

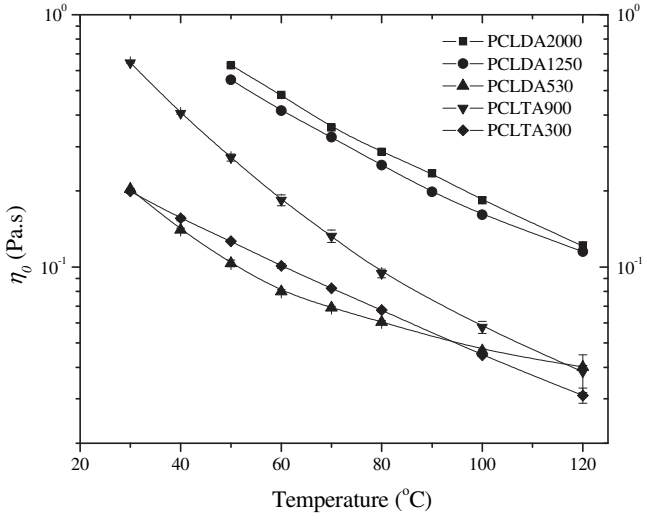

Fig. 4. Temperature dependence of zero-shear viscosity for PCLAs.

PCLTA900. PCLA networks did not swell in water or PBS, suggesting the scaffolds made from them can remain the original shape in *in vivo* implantation before the degradation starts to be apparent.

3.3. Thermal properties

DSC curves in Fig. 5 from the heating run were used to obtain the thermal properties of PCLAs such as T_g, T_m, and the heat of fusion ΔH_m listed in Table 1. T_g was determined using the midpoint temperature of the glass transition and T_m was the highest peak temperature among multiple exothermal peaks, which corresponded to the different arm lengths in PCL precursors and PCLAs. Crystallinity χ_c was calculated using the equation of $\chi_c = [\Delta H_m/(\phi_{PCL}\Delta H_m^c)] \times 100\%$, where ΔH_m^c of completely crystalline PCL is 135 J/g [38] and ϕ_{PCL} was 90.1%, 96.3%, 96.9%, and 91.8% for PCLDA530, 1250, 2000, and PCLTA900, respectively.

Like their PCL diol precursors, PCLDAs were all semi-crystalline with varied T_m and crystallinity. PCLDA530, 1250, and 2000 had a T_m at 22.9, 46.1, 49.1 °C and crystallinity of 33.2%, 50.9%, 55.1%, respectively. Because of their low-molecular weights, PCL triol300 and PCLTA300 were amorphous with a T_g at −65.5 and −70.5 °C, respectively. PCL triol900 and PCLTA900 were semi-crystalline with three melting peaks at 15, 23, and 29 °C. After crosslinking, crystallinity and T_m decreased significantly for all PCLAs because the crystallization of PCL segments was strongly restricted by the polymer network [25,39]. As demonstrated in Fig. 4, crosslinked PCLDA530, PCLTA300 and 900 became completely amorphous. In contrast, crosslinked PCLDA1250 and 2000 were still semi-crystalline with a lower T_m of 34.8 and 39.2 °C and a reduced crystallinity of 29.3% and 33%, respectively. These five crosslinked PCLAs with varied crosslinking density, χ_c, and T_m therefore served excellent model polymers with distinct mechanical properties at both room temperature and 37 °C.

Correspondingly, WAXD patterns in Fig. 6 demonstrate the crystalline structures of PCL precursors, uncrosslinked and crosslinked PCLAs. PCLAs shared the same diffraction peaks at $2\theta = 20.2$, 21.4, 22.0, 23.7, and 30.0° with their precursor PCL diols, corresponding to the *d*-spacings of 0.440, 0.415, 0.403, 0.375, and 0.295 nm, respectively [25,40]. After crosslinking, the diffraction peak at $2\theta = 22.0°$ was no longer prominent for all five crosslinked PCLAs and there was only a broad diffraction peak at $2\theta = 20.2°$ ($d = 0.440$ nm) for crosslinked PCLDA530 and PCLTA300, confirming their amorphous characteristics.

TGA was performed to determine the thermal stability of both uncrosslinked and crosslinked PCLAs as well as their PCL precursors. As demonstrated in Fig. 7, all samples had one single degradation step. The onset thermal degradation temperature (T_d) increased significantly after the acrylation of PCL precursors, especially for the low-molecular-weight ones, because thermal crosslinking occurred before degradation in the measurements. T_d increased slightly further for all three PCLAs after crosslinking. It should be noted that T_d was much lower than the reported values of over 600 °C for the same PCL networks synthesized using the previous method [19]. T_d for crosslinked PCLDA530, 1250, and 2000 and PCLTA300 and 900 in this study was 407, 412, 414, 402, and 404 °C, respectively. In comparison, the values for their uncrosslinked counterparts were 393, 405, 406, 368, and 405 °C.

3.4. Mechanical and rheological properties of crosslinked PCLAs

Rheological properties of crosslinked PCLAs at 25, 37, and 60 °C measured using dynamic frequency sweep mode are demonstrated

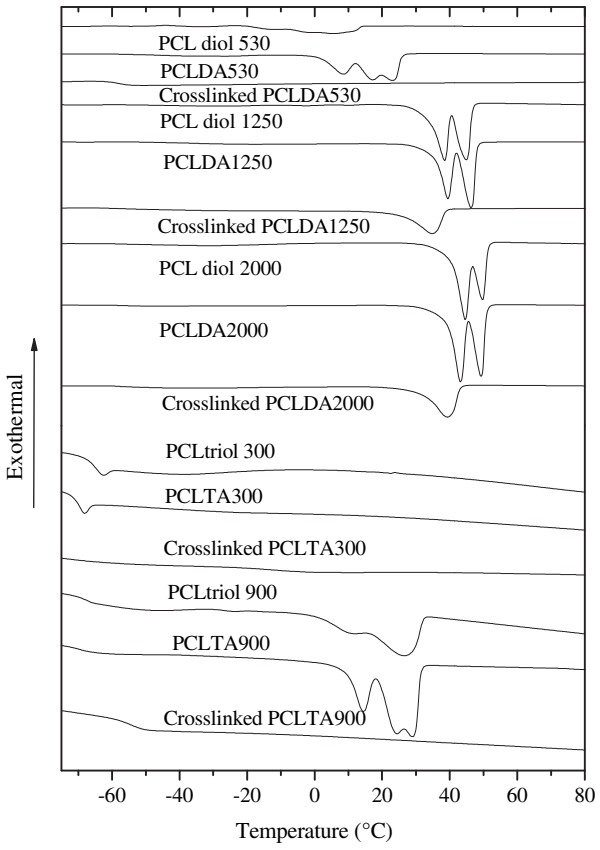

Fig. 5. DSC curves of PCL precursors, PCLAs, and crosslinked PCLAs.

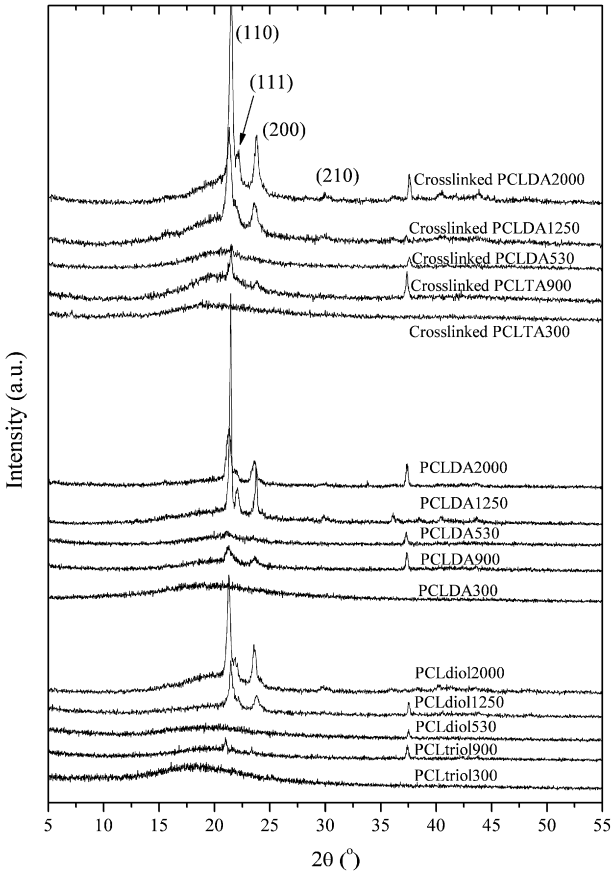

Fig. 6. WAXD patterns of PCL precursors, PCLAs, and crosslinked PCLAs.

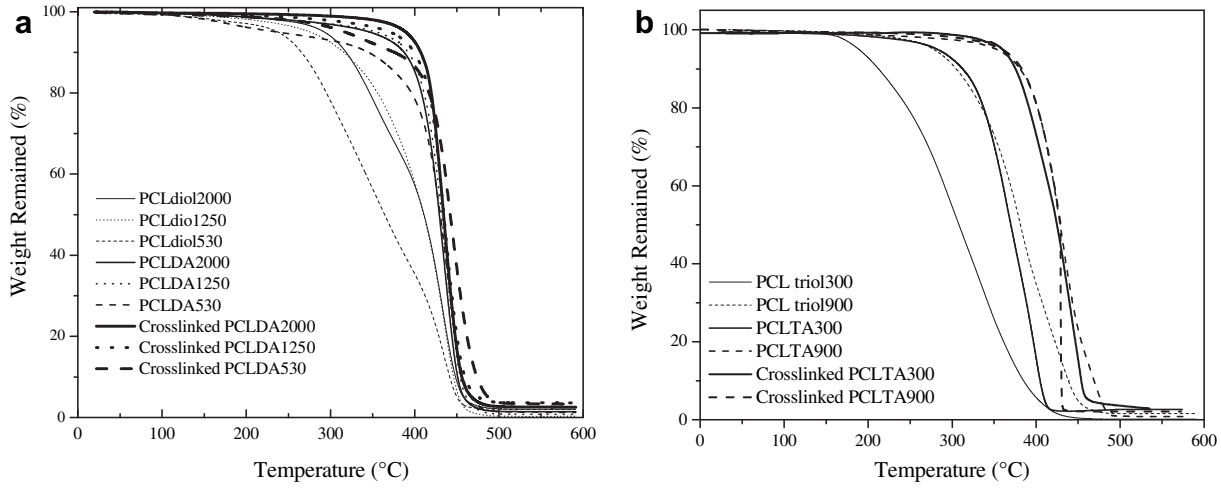

Fig. 7. TGA curves of (a) PCL diols, PCLDAs, and crosslinked PCLDAs and (b) PCL triols, PCLTAs, and crosslinked PCLTAs.

in Fig. 8. All crosslinked PCLAs showed characteristic curves as polymer networks by showing that frequency-independent G' was always greater than G'' and shear thinning (approximately $\eta \sim \omega^{-1}$) occurred for η [41]. Because crosslinked PCLDA530 was amorphous, there was no variance with temperature for G', G'', and η. In contrast, both crosslinked PCLDA1250 and 2000 showed distinct sets of curves at different temperatures as their crystallinity changed with temperature. With the enhancement of crystalline domains, G' at 1 rad/s increased from 0.854 MPa for amorphous crosslinked PCLDA530 to 13.04 MPa and further to 53.9 MPa for semi-crystalline crosslinked PCLDA1250 and 2000 at 25 °C, respectively. When the networks were all amorphous at 60 °C, G' at

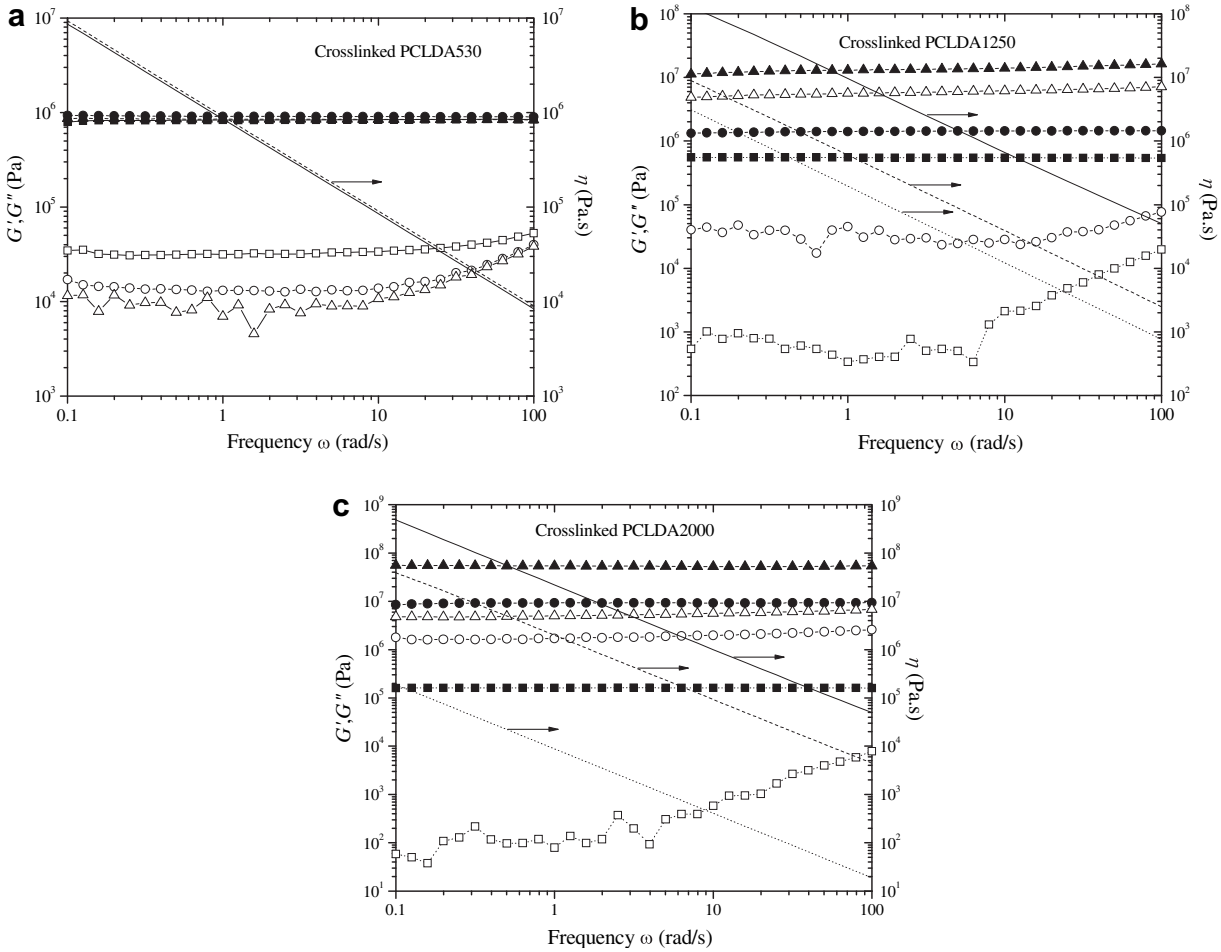

Fig. 8. Storage modulus G' (solid symbols), loss modulus G'' (open symbols), and viscosity η (lines) vs. frequency for crosslinked PCLDAs (a: PCLDA530; b: PCLDA1250; c: PCLDA2000) at 25 °C (triangles and solid lines), 37 °C (circles and dashed lines), and 60 °C (squares and dotted lines).

Table 2
Mechanical properties of crosslinked PCLAs at 37 °C.

Polymer	Compression modulus (MPa)	Shear modulus (MPa)	Torsional modulus (MPa)	Tensile modulus (MPa)
PCLDA530	6.38 ± 0.63 (8.5 ± 1.0)[a]	0.98	6.64	5.98 ± 0.61 (8.3 ± 1.0)[a]
PCLDA1250	14.5 ± 2.17 (89.5 ± 15.6)[a]	1.34	8.52	21.5 ± 4.99 (118 ± 20)[a]
PCLDA2000	49.3 ± 5.92 (124 ± 21.5)[a]	9.23	10.8	70.0 ± 31.1 (290± 54)[a]
PCLTA300	8.83 ± 0.75 (10.1 ± 1.6)[a]	2.01	7.78	23.2 ± 1.14 (26.9 ± 6.5)[a]
PCLTA900	6.06 ± 0.59 (6.9 ± 0.4)[a]	1.00	1.16	4.84 ± 0.47 (6.6 ± 1.2)[a]

[a] Data in parenthesis were obtained at room temperature.

1 rad/s decreased from 0.832 MPa for crosslinked PCLDA530 to 0.551 MPa for crosslinked PCLDA1250 and 0.162 MPa for crosslinked PCLDA2000. Shear modulus for an amorhpus polymer network is determined by the average molecular weight (M_c) between two neighboring crosslinks through the equation $G = \rho RT/M_c$, where ρ is the density [42]. In this study, M_c was the molecular weight of PCL diol in PCLDAs and was the arm molecular weight in PCLTAs. Similar to crosslinked PCLDA530 in Fig. 8a, crosslinked PCLTAs were amorphous and did not show temperature dependence in G', G'', and η (not shown). Crosslinked PCLTA300 had higher rheological values compared with crosslinked PCLTA900 as it was a denser network. For example, shear modulus (Table 2) was 2.01 MPa for the former but only 1.00 MPa for the later.

The mechanical properties of crosslinked PCLA disks or strips determined from tensile, compression, shear, and torsional measurements at 37 °C are shown in Table 2 and representative stress-strain curves of these five samples in tensile and compressive measurements are demonstrated in Fig. 9. Because crosslinked PCLDA530, PCLTA300 and 900 were amorphous without the enhancement of crystallites, their mechanical properties were determined by crosslinking density. Therefore all the moduli of crosslinked PCLDA530 were the lowest among crosslinked PCLDAs and the moduli of crosslinked PCLTA300 were always higher than those of crosslinked PCLTA900. With crystallites serving as physical fillers and forming a physical network, crosslinked PCLDA2000 with the highest crystallinity and T_m had the highest tensile, shear, compression, and torsional moduli at 37 °C among these samples. When the measurement was performed at room temperature, mechanical properties increased slightly for amorphous samples, crosslinked PCLDA530 and PCLTAs. For semi-crystalline samples, the crystalline domains melted partially at 37 °C although their T_m was higher than it. As the result, when the measurement temperature was lowered from 37 to 25 °C, tensile moduli increased greatly from 21.5 and 70.0 MPa to 118.4 and 289.6 MPa while compression moduli increased from 14.5 and 49.3 MPa to 89.5 and 124.4 MPa for PCLDA1250 and 2000, respectively. From the above results, it is evident that mechanical properties of crosslinked PCLAs can be well modulated in a wide range through both crosslinking density and crystallinity.

3.5. Surface characteristics and protein adsorption

Surface characteristics of crosslinked PCLDAs such as morphology, hydrophilicity, and the capability of adsorbing protein from cell culture medium have been determined. SEM images of the surfaces of crosslinked PCLDA530 and 2000 disks are shown in Fig. 10. Because of the higher gel fractions, both crosslinked PCLDA530 and 2000 as well as other three crosslinked PCLAs had smooth surfaces after being purified in acetone, compared with the rough surfaces in crosslinked PCLFs, especially crosslinked PCLF2000 having the lowest gel fraction of 0.53 [7,25]. However, AFM images in Fig. 11 still demonstrate difference in surface morphology at nanometer scale. Semi-crystalline samples, i.e. crosslinked PCLDA1250 and 2000 had rougher surfaces (RMS roughness: 204 and 260 nm) than amorphous crosslinked PCLDA530 (RMS roughness: 8.6 nm) due to their comparably lower gel fractions and surface rearrangement from purification in acetone and then crystallization. In order to clarify the role of surface morphology in influencing cell responses, we deliberately compressed disks of crosslinked PCLDA1250 and 2000 and achieved smoother surfaces (Fig. 11) with lower RMS roughnesses of 20.8 and 53.8 nm, respectively.

The fabrication method using photo-crosslinking [7] was efficient for making nerve conduits free of defects, as shown in Fig. 10c. Because the T_m of PCLDA2000 was higher than 37 °C, nerve conduits made from it had sufficient flexibility and resistance to tear during *in vivo* implantation while the suturability was also excellent to satisfy the basic requirements of being used for guided nerve regeneration [7,8]. The flexural modulus of PCLDA2000

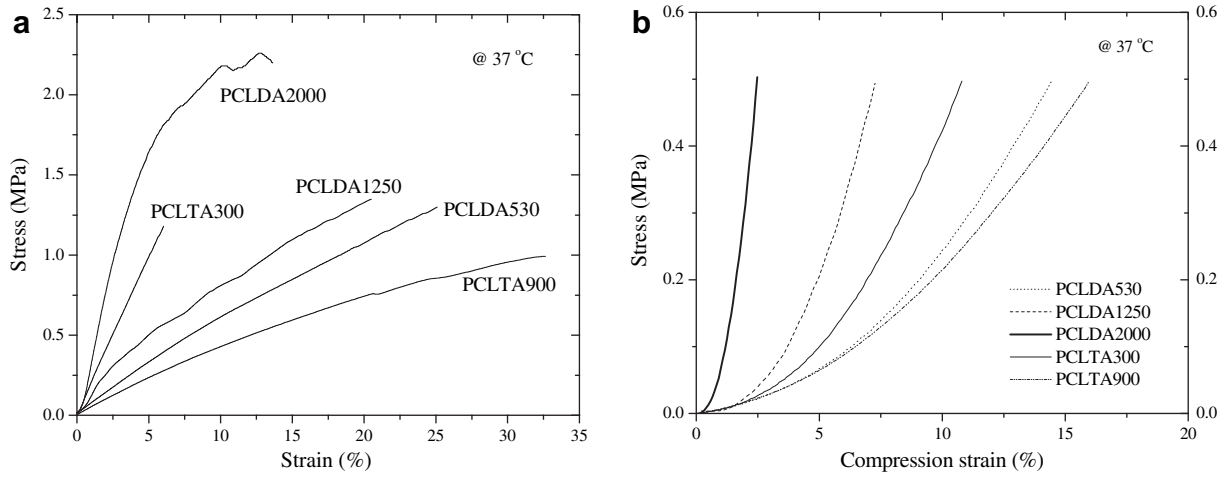

Fig. 9. Tensile (a) and compression (b) stress-strain curves of crosslinked PCLAs at 37 °C.

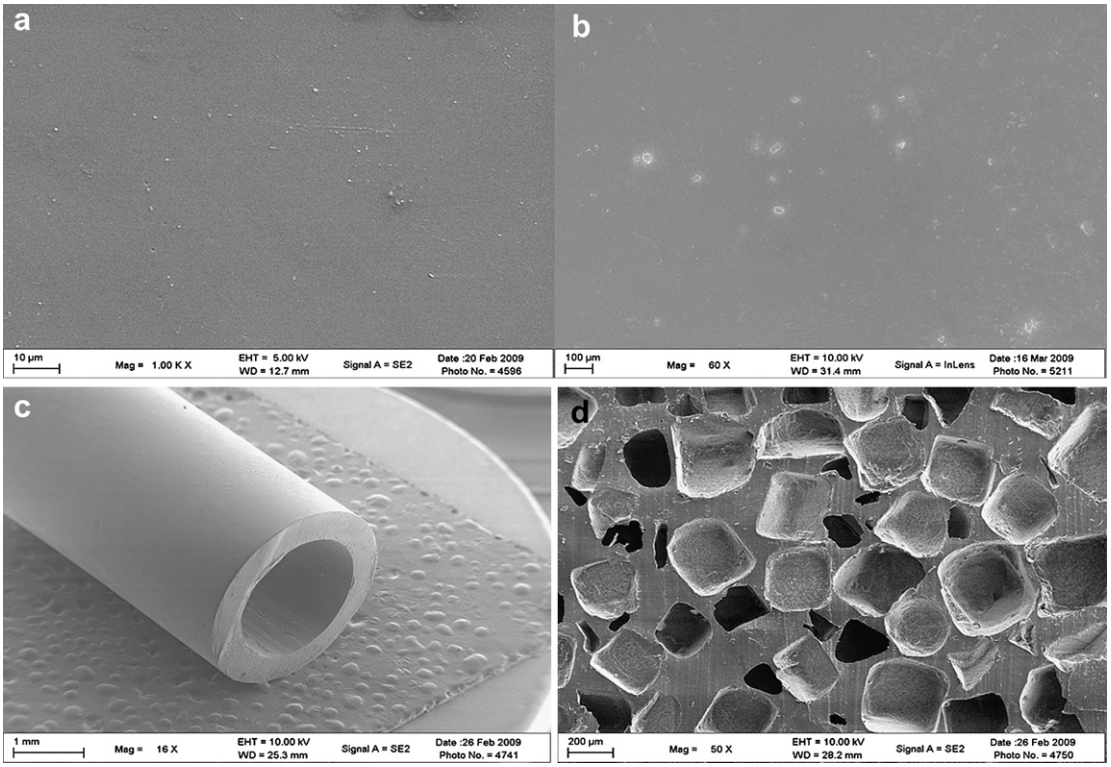

Fig. 10. SEM images of (a) crosslinked PCLDA530 and (b) PCLDA2000 disks, cross-sections of (c) a crosslinked PCLDA2000 conduit and (d) a crosslinked PCLDA2000 porous scaffold.

conduits was 64 MPa at room temperature. Fig. 10d shows that salt leaching method could also be applied to prepare scaffolds with controllable porosity and pore size for bone-tissue-engineering applications. Presently we are fabricating nerve conduits and bone scaffolds using these PCLAs and stereolithographic methods.

Fig. 12 shows the contact angles of water on the surfaces of crosslinked PCLAs and the surfaces' capability of adsorbing serum proteins from cell culture medium. The contact angle of water increased from $59 \pm 5^\circ$ on crosslinked PCLDA530 to $67 \pm 3^\circ$ and $77 \pm 4^\circ$ on crosslinked PCLDA1250 and 2000, respectively. It indicated a higher hydrophobicity when the polymer was more crystalline, as reported earlier for crosslinked PCLFs [7]. For amorphous crosslinked PCLTA300 and 900, the contact angle of water was $56 \pm 4^\circ$ and $52 \pm 3^\circ$, respectively. Aqueous adhesion tension (τ) calculated from the water contact angle α using the equation of $\tau = \gamma_{lv}\cos\alpha$ and water-vapor surface tension γ_{lv} of 72.8×10^3 N/m [30] was 3.75 ± 0.51, 2.78 ± 0.18, 1.61 ± 0.27, 4.46 ± 0.3, and 4.03 ± 0.41 N/m for crosslinked PCLDA530, 1250, 2000, PCLTA300 and 900, respectively. Both hydrophilicity and surface roughness influence the capability of a polymer surface to adsorb proteins from culture medium [30–32]. Though a higher roughness was observed from crosslinked PCLDA2000 disks (Fig. 11), its higher hydrophobicity might prohibit culture medium from spreading over the disk surface. Crosslinked PCLDA1250 disks had advantages of both surface roughness and comparably lower hydrophobicity, therefore they had the highest capability of adsorbing proteins

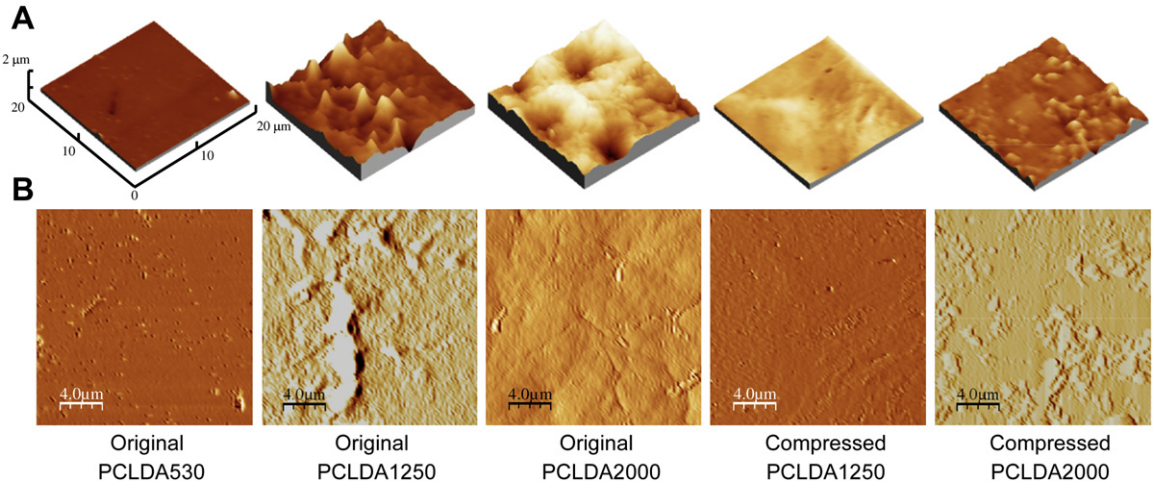

Fig. 11. AFM images (A: 3D height images; B: 2D phase images) of original crosslinked PCLDA disks and compressed disks of crosslinked PCLDA1250 and 2000.

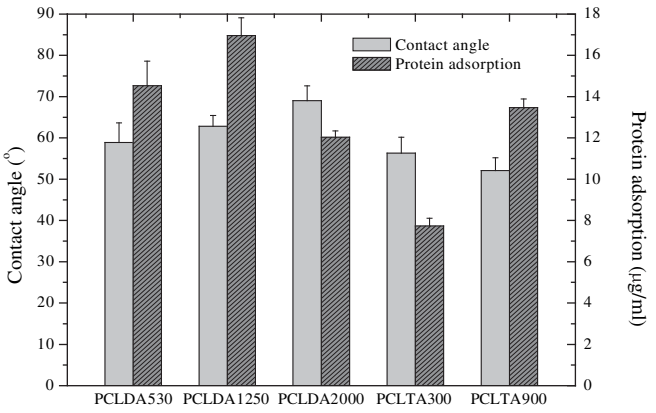

Fig. 12. Contact angles of water and protein adsorption on crosslinked PCLA disks.

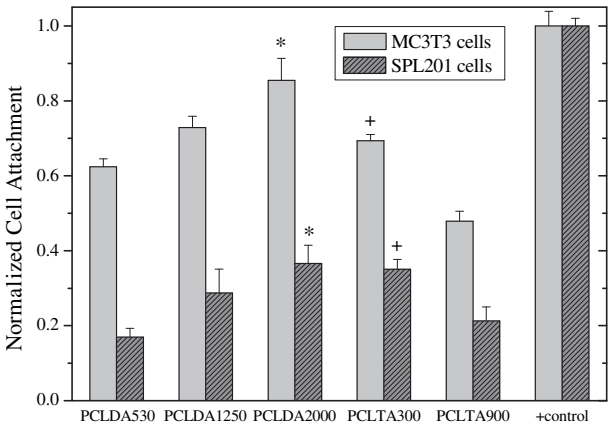

Fig. 13. Normalized MC3T3 and SPL201 cell attachment 4 h post-seeding on crosslinked PCLA disks, compared with cell-seeded tissue-culture polystyrene (TCPS) as positive control. $^{*}p < 0.05$ relative to PCLDA530, PCLDA1250, and TCPS. $^{+}p < 0.05$ relative to PCLTA900 and TCPS.

from culture medium. This observation was in good agreement with our earlier report on the protein adsorption on three crosslinked PCLFs [7]. Crosslinked PCLTA900 disks could adsorb more proteins than crosslinked PCLTA300 although both disks were amorphous and had similar water contact angle of ~55°.

3.6. Cell viability, attachment, spreading, and proliferation

Because PCLAs were synthesized for bone and nerve tissue-engineering applications, both mouse MC3T3 and rat SPL201 cells were chosen to evaluate cell viability and responses to the polymer disks. Similar to PCLF networks [7,24], no detectable degradation could be observed for all PCLA networks in PBS at 37 °C in one week. Therefore, surface morphology and mechanical properties largely remained in the duration for cell studies. All crosslinked PCLAs demonstrated no cytotoxicity in 4 and 7 days (Fig. S3) for MC3T3 and SPL201 cells, respectively. Cell proliferation was performed in the same duration for each cell type and cell attachment was evaluated 4 h post-seeding.

Cell attachment and spreading on polymer substrata are crucial for cell motility, growth, and organization of tissues when polymers are used in biomedical applications [43]. It can be seen in Fig. 13 that the normalized number of attached cells 4 h post-seeding increased from crosslinked PCLDA530 to 1250 and 2000 while it decreased from crosslinked PCLTA300 to 900 consistently for both cell types. MC3T3 cells attached on the polymer surfaces significantly more than SPL201 cells, suggesting different cells may respond distinctly to the same substrates because of the distinct mechanical characteristics of their original tissues [34]. However, these two cell types might have different activities as they were obtained from different sources and passages. MC3T3 cell area at day 1 post-seeding was $1503 \pm 320\ \mu m^2$ per cell on the disks of crosslinked PCLDA530 and it did not increase significantly with culture time. In contrast, cell area at day 1 increased to 1873 ± 168 and $2108 \pm 305\ \mu m^2$ per cell on crosslinked PCLDA1250 and 2000, respectively. Similar to crosslinked PCLDA530, another two amorphous polymer networks, crosslinked PCLTA300 and 900 had values of 1704 ± 315 and $1609 \pm 229\ \mu m^2$ per cell, respectively.

As demonstrated in Fig. 14A, the number of MC3T3 cells increased significantly when the substrate changed from crosslinked PCLDA530 to 1250 and 2000 at day 1, 2, and 4 post-seeding. It decreased when the substrate changed from crosslinked PCLTA300 to 900. The trend was in agreement with cell attachment in Fig. 13. Attached MC3T3 cells demonstrated spread-out phenotype. Fig. 14B shows the cell numbers on the substrates at different time points, which were calculated from the MTS absorption data and the standard curve constructed using positive wells with five known cell numbers of 5, 10, 20, 30, and 50×10^3 4 h post-seeding. The data and trend in Fig. 14B were consistent with the cell images in Fig. 14A. Substantial cell proliferation could be found on the disks of crosslinked PCLDA2000 while it was weaker on the disks of crosslinked PCLDA1250 and 530. Proliferation index (PI) was calculated by dividing the cell number at day 4 by the initial number of attached cells 4 h post-seeding (Fig. 13) [44]. It increased from 1.25 on crosslinked PCLDA530 to 1.53 and 1.64 on crosslinked PCLDA1250 and 2000, respectively. Doubling time of cells was also determined by plotting the natural log of the cell number against time, from which the growth rate was obtained as the slope or ln(PI)/4, and the following equation: doubling time = ln2/growth rate [45]. Doubling time decreased from 9.25 days on crosslinked PCLDA530 to 5.25 days on crosslinked PCLDA1250 and further to 4.24 days on crosslinked PCLDA2000, indicating faster cell proliferation on more crystalline polymer networks. These observations were consistent with the earlier report on the cell responses to crosslinked PCLFs using rat BMSCs and SPL201 cells [7,26]. For amorphous disks of crosslinked PCLTA300 and 900, no cell proliferation existed although sparse cells with less spread-out phenotype could be observed on their surfaces.

In Fig. 14C and D, the above trend could also be observed using SPL201 cells although the numbers of cells were evidently lower. Crosslinked PCLDA2000 had significantly higher cell numbers at day 1, 4, and 7 post-seeding and it could support cell proliferation with a PI of 4.84. In contrast, crosslinked PCLDA1250 with a semi-crystalline structure could support cell proliferation with a lower PI of 4.44. However, the doubling time of SPL201 cells was 3.08 and 3.26 days on crosslinked PCLDA2000 and 1250, respectively. Amorphous crosslinked PCLDA530 and PCLTA300 and 900 could not support SPL201 cell proliferation and there was even a decrease in cell numbers after SPL201 cells attached initially on the disks. Furthermore, attached SPL201 cells demonstrated round-shaped phenotype without extensive spreading on these amorphous disks.

3.7. Further discussion on cell–material interactions

In agreement with the earlier findings using PCLF networks [7,25,26], it is evident that PCLA networks with controllable mechanical properties by varying crystallinity can result in dramatically different cell responses. Generally there are three major categories of determining factors for cell–material interactions [30–32]. Chemical factors include functional groups on surface, surface hydrophilicity, charge density, the capability of adsorbing protein,

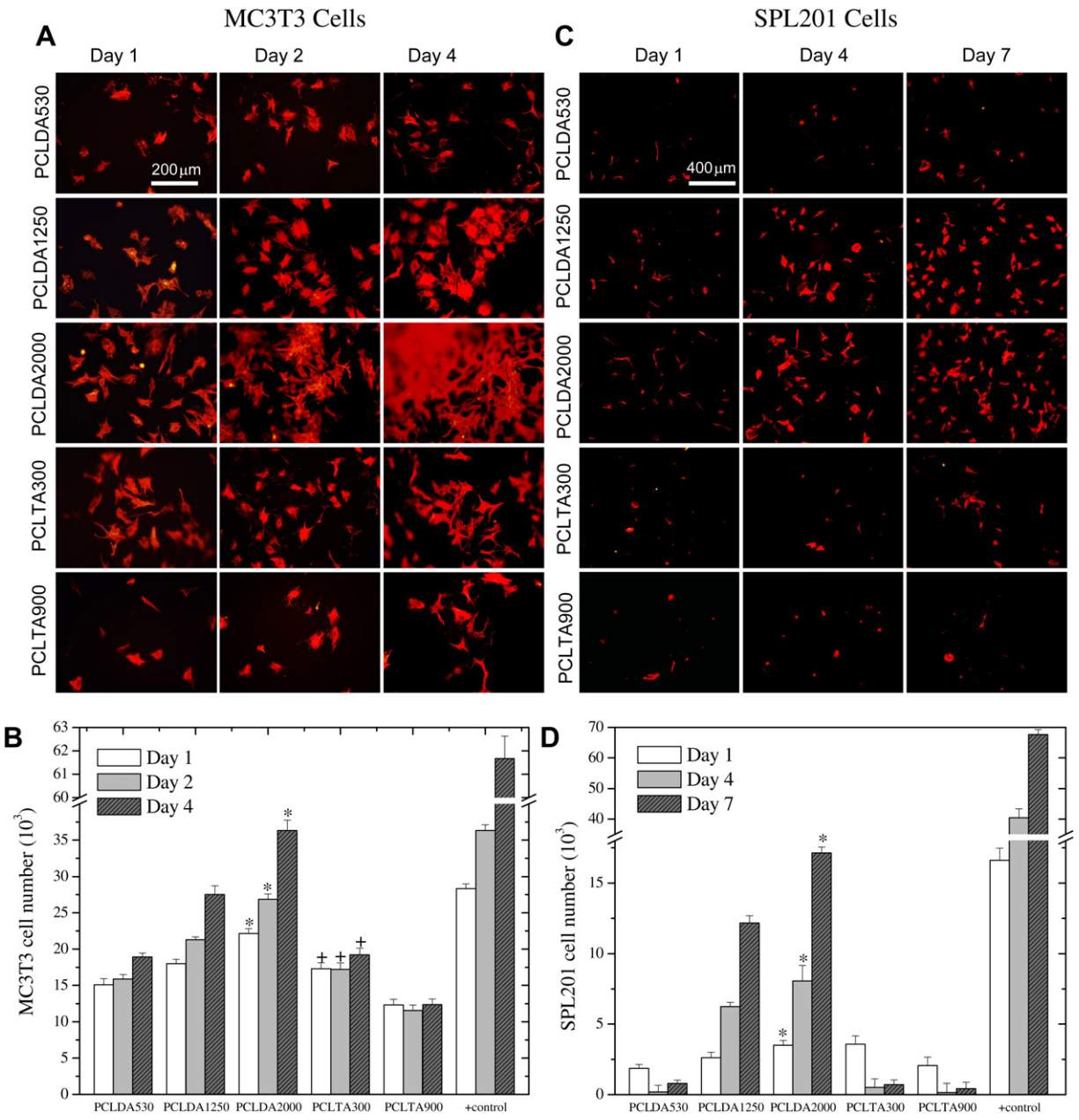

Fig. 14. Morphology of mouse MC3T3 cells (A: ×200) and rat SPL201 cells (C: ×100) on crosslinked PCLA disks at day 1, 2, and 4, and at day 1, 4, and 7 post-seeding, respectively. The scale bar of 200 and 400 μm is applicable to all in A and C, respectively. Corresponding numbers of MC3T3 cells (B) and SPL201 cells (D) on the crosslinked PCLA disks, compared with cell-seeded TCPS as positive (+) control. $^{*}p < 0.05$ relative to PCLDA530, PCLDA1250 and TCPS. $^{+}p < 0.05$ relative to PCLTA900 and TCPS.

and protein coating [30–32]. Topological features and surface roughness at both micron and nanometer scales will influence cell attachment and proliferation because of contact guidance effect and increased surface area [30–32]. Mechanical factors such as surface stiffness and hydrodynamic shear stress applied onto cells will influence cell proliferation and phenotype significantly as the actin-myosin associations can be considered as probes to detect the mechanical signals and transduce them to the nucleus [30–35]. Consequently, Ca^{2+} influx across the cell membrane can be modulated by the nucleus to regulate cell responses including cell motility, spreading, proliferation, and apoptosis [30–35].

All crosslinked PCLAs were composed of PCL dominantly without being chemically modified on the surfaces. Nevertheless, as discussed in Section 3.4, surface chemistry such hydrophilicity and the capability of adsorbing protein from cell culture medium varied as the polymer crystallinity changed. Hydrophilicity, or surface energy, can dictate protein adsorption and conformation [45]. Low surface energy and hydrophobicity generally result in increased protein adsorption [45]. Although it is often believed that better protein adsorption and intermediate wettability with a water contact angle of ~50° may help cell attachment and proliferation [30–32], clear correlation between them is not universal without exceptions [7,24,26,46]. Surface rearrangement induced by water contact might not exist in the present crosslinked PCLAs as hydrophobic polymer networks resist this change. As discussed earlier in Fig. 10, crosslinked PCLDA2000 had the highest contact angle because of its highly crystalline characteristics and the lowest protein adsorption from culture medium among these crosslinked PCLAs. It is worthwhile to note and also was suggested by previous studies [45,47], the amount of adsorbed proteins might not be the only indicator in

affecting cell affinity since they might adopt different conformations on the surfaces and their functionalities could be different. Moreover, non-extracellular matrix (ECM) proteins such as albumin and ECM proteins for supporting cell adhesion such as fibronectin should be differentiated from each other in total adsorbed proteins [30,32]. Such concerns are presently under investigations in our laboratory. Nevertheless, both hydrophilicity and protein adsorption cannot interpret why crosslinked PCLDA2000 could support cell attachment and proliferation significantly better than other less crystalline or amorphous crosslinked PCLAs.

Using PLLA with a T_g higher than 37 °C, researchers could prepare specimens with well modulated crystallinity by quenching the sample from melt and then crystallizing at different temperatures between T_g and T_m [48,49]. Differences in cell behavior were reported on amorphous or less crystalline versus more crystalline PLLA substrates [48,49]. The influence of nanometer scale roughness on proliferation was also revealed on the osteoblast response to PLLA crystallinity [50,51]. However, the origins for different cell behaviors still remain elusive after systematic investigations on numerous factors by Park and Griffith [48], especially when the surface morphology is not involved in samples with smooth surfaces. Although crosslinked PCLDA1250 and 2000 were semi-crystalline, their T_gs ranged from −70 °C to −50 °C and the preparation method of photo-crosslinking between two smooth glass plates constrained crystallizable PCL segments from forming crystallite-induced surface features at length scale smaller than that demonstrated in Fig. 11. In order to elucidate the role of surface roughness in influencing cell attachment and proliferation, crosslinked PCLDA1250 and 2000 disks were melted and compressed between two glass plates and then cooled down below their T_m to obtain smoother disks. By comparing the cell numbers at 4 h, 1 and 4 days post-seeding, little difference was found in cell attachment and proliferation between original and compressed disks for both crosslinked PCLDA1250 and 2000 (Fig. S4). This result indicated that surface morphology might not be responsible for the dramatic difference in cell responses shown in Figs. 13 and 14.

Unlike glassy PLLA having mechanical properties with little dependence on crystallinity at 37 °C [52], PCL crystalline domains formed a second network to strengthen the amorphous chemical network dramatically. Therefore, the role of crystalline structure in determining cell responses to these two crystalline polymers may be fundamentally different. Though more investigations need to be performed, we tentatively attribute the enhanced cell attachment, spreading, and proliferation on semi-crystalline PCLDA2000 network to the mechanical factor. There remain a few unanswered questions involving the threshold for a polymer surface to be sufficiently stiff to support a certain cell type to attach, spread, and proliferate. We explore to quantify the cell–material interactions by directly measuring cell adhesion force on this series of polymers using tools such as micropipette peeling, hydrodynamic shear stress, and centrifugation [53].

Based on these polymers with tunable mechanical properties and cell responses, we can select suitable biomaterials and develop better ones for different applications ranging from hard tissue replacement to soft tissue replacement and enhance our understanding about the materials' role in tissue-repair strategies. Mechanical properties can be further modulated in a wider range by blending different crosslinkable PCLAs at different ratios or with amorphous crosslinkable polymer poly(propylene fumarate) (PPF) that has a higher density of crosslinkable segments [17,24]. Long-period biocompatibility of PCLA networks in medical applications will be strongly influenced by the degradation and crystallinity. By incorporating with hydrophilic dangling chains with positive charges, the wettability and biocompatibility of PCLA networks can be improved without sacrificing mechanical properties significantly. As these PCLAs can be crosslinked thermally or by photo-initiation, they can be fabricated into 3D structures such as nerve conduits with structural features such as a porous wall and multiple guiding channels. Using this series of PCLAs, we are also studying the role of crystalline domains in controlling mouse PC12 and neuroprogenitor cell differentiation in the presence of nerve growth factor on 2D substrates, and MC3T3 cell migration and proliferation in 3D porous scaffolds.

4. Conclusions

A facile synthetic route has been applied to prepare crosslinkable poly(ϵ-caprolactone) acrylates (PCLAs) including three poly(ϵ-caprolactone) diacrylates (PCLDAs) and two poly(ϵ-caprolactone) triacrylates (PCLTAs) in the presence of a new proton scavenger, K_2CO_3. Besides more convenient synthesis and purification steps, the light-colored products yielded using this new method were more efficient for photo-crosslinking and cell studies. Crosslinked PCLAs in the present study were excellent model polymeric systems with chemically-crosslinked network and physical network connected by crystalline domains. Through varying the molecular weight of PCL precursor, crystallinity and T_m could be well modulated. Consequently, their mechanical and rheological properties, surface roughness and hydrophilicity varied significantly. Among these five PCLAs, PCLDA530 and PCLTA300 had sufficiently low viscosities for being used as resins in stereolithography to fabricate polymer scaffolds directly. Photo-crosslinked PCLDA2000 substrate with the highest crystallinity and mechanical properties was the most favorable material for cell attachment, spreading, and proliferation using both mouse MC3T3 cells and rat SPL201 cells. Surface morphology and other chemical cues such as hydrophilicity and the capability of adsorbing protein could not be applied to interpret the trend in cell responses to the crosslinked PCLA disks. Tentatively, surface stiffness enhanced by the crystalline domains was used to explain why cell attach and proliferate most significantly on crosslinked PCLDA2000 disks. Together with excellent cytocompatibility, these polymers were used to fabricate 2D disks, 3D tubes and scaffolds using photo-crosslinking, demonstrating their potentials as injectable biomaterials for diverse tissue-engineering applications.

Acknowledgements

This work was supported by the start-up fund of the University of Tennessee. We thank Xueguang Jiang, Xiaoming Jiang, and Dr. Bin Zhao in the Department of Chemistry for the help with GPC and contact angle measurements, Dr. Joseph E. Spruiell in our department for WAXD diffraction measurements, Dr. Stephen Jesse at Oak Ridge National Laboratory for AFM measurements, and Dr. Anthony J. Windebank and Jarred Nesbitt at Mayo Clinic for supplying SPL201 cells.

Appendix. Supplementary information

The supplementary data associated with this article can be found in the on-line version at doi:10.1016/j.polymer.2009.11.042.

References

[1] Domb AJ, Kost J, Wiseman D. Handbook of biodegradable polymers. Amsterdam: Harwood Academic Publishers; 1997.
[2] Guelcher SA, Hollinger JO. Introduction to biomaterials. Boca Raton: CRC Press; 2005.
[3] Peter SJ, Miller MJ, Yasko AW, Yaszemski MJ, Mikos AG. J Biomed Mater Res 1998;43(4):422–7.

[4] Khan Y, Yaszemski MJ, Mikos AG, Laurencin CT. J Bone Joint Surg Am 2008;90A(S1):36–42.
[5] Lee KW, Wang S, Lu L, Jabbari E, Currier BL, Yaszemski MJ. Tissue Eng 2006;12(10):2801–11.
[6] Lee KW, Wang S, Fox B, Ritman EL, Yaszemski MJ, Lu L. Biomacromolecules 2007;8(4):1077–84.
[7] Wang S, Yaszemski MJ, Knight AM, Gruetzmacher JA, Windebank AJ, Lu L. Acta Biomater 2009;5(5):1531–42.
[8] Schmidt CE, Leach JB. Annu Rev Biomed Eng 2003;5:293–347.
[9] Heath CA, Rutkowski GE. Tibtech 1998;16(4):163–8.
[10] Kannan RY, Salacinski HJ, Butler PEM, Seifalian AM. Biotechnol Appl Biochem 2005;41:193–200.
[11] Meek MF, Coert JH. Ann Plast Surg 2008;60(4):466–72.
[12] Belkas JS, Shoichet MS, Midha R. Neurol Res 2004;26:151–60.
[13] Rubinstein M, Colby RH. Polymer physics. New York: Oxford; 2003. p. 199.
[14] Anseth KS, Shastri VR, Langer R. Nature Biotechnol 1999;17:156–9.
[15] Fisher JP, Dean D, Engel PS, Mikos AG. Annu Rev Mater Res 2001;31:171–81.
[16] Ifkovits JL, Burdick JA. Tissue Eng 2007;13:2369–95.
[17] Turunen MPK, Korhonen H, Tuominen J, Seppala JV. Polym Int 2001;51:92–100.
[18] Wang S, Lu L, Yaszemski MJ. Biomacromolecules 2006;7(6):1976–82.
[19] Kweon HY, Yoo MK, Park IK, Kim TH, Lee HC, Lee HS, et al. Biomaterials 2003;24:801–8.
[20] Lee K-S, Kim DS, Kim BS. Biotechnol Bioprocess Eng 2007;12:152–6.
[21] Chung I, Xie D, Puckett AD, Mays JW. Eur Polym J 2003;39:1817–22.
[22] Jabbari E, Wang SF, Lu LC, Gruetzmacher JA, Ameenuddin S, Hefferan TE, et al. Biomacromolecules 2005;6:2503–11.
[23] Wang S, Lu L, Gruetzmacher JA, Currier BL, Yaszemski MJ. Biomaterials 2006;27:832–41.
[24] Wang S, Kempen DH, Simha NK, Lewis JL, Windebank AJ, Yaszemski MJ, et al. Biomacromolecules 2008;9:1229–41.
[25] Wang S, Yaszemski MJ, Gruetzmacher JA, Lu L. Polymer 2008;49:5692–9.
[26] Wang S, Kempen DH, Yaszemski MJ, Lu L. Biomaterials 2009;30:3359–70.
[27] Wang S, Lu L, Gruetzmacher JA, Currier BL, Yaszemski MJ. Macromolecules 2005;38(17):7358–70.
[28] Perrin DE, English JP. Polycaprolactone. In: Domb AJ, Kost J, Wiseman D, editors. Handbook of biodegradable polymers. Amsterdam: Harwood Academic Publishers; 1997.
[29] Cai L, Wang S. Biomacromolecules, in press.
[30] Harbers GM, Grainger DW. Cell–material interactions: fundamental design issues for tissue engineering and clinical considerations. In: Guelcher SA, Hollinger JO, editors. Introduction to biomaterials. Boca Raton: CRC Press; 2005. p. 15–45.
[31] Wong JY, Leach JB, Brown XQ. Surf Sci 2004;570:119–33.
[32] Saltzman WM, Kyriakides TR. Cell interactions with polymers. In: Lanza R, Langer R, Vacanti J, editors. Principles of tissue engineering. 3rd ed. San Diego: Elsevier Academic Press; 2007. p. 279–96.
[33] Pelham RJ, Wang Y-L. Proc Natl Acad Sci USA 1997;94:13661–5.
[34] Discher DE, Janmey P, Wang YL. Science 2005;310:1139–43.
[35] Pelham RJ, Wang Y-L. Biol Bull 1998;194:348–9.
[36] Rubinstein M, Colby RH. Polymer physics. New York: Oxford; 2003. p. 337.
[37] Gimenez J, Cassagnau P, Fulchiron R, Michel A. Macromol Chem Phys 2000;201:479–90.
[38] Brandrup J, Immergut EH, editors. Polymer handbook. 3rd ed. New York: Wiley; 1989.
[39] Mandelkern L. Crystallization of polymers. 2nd ed., vol. 1. New York: McGraw-Hill; 2001 [chapter 7].
[40] Bittiger H, Marchess RH, Niegisch WD. Acta Cryst 1970;B26:1923–7.
[41] Rubinstein M, Colby RH. Polymer physics. New York: Oxford; 2003. p. 293.
[42] Sperling LH. Introduction to physical polymer science. 3rd ed. New York: Wiley; 2001. pp. 363–431.
[43] Gumbiner BM. Cell 1996;84:345–57.
[44] Shin H, Zygourakis K, Farach-Carson MC, Yaszemski MJ, Mikos AG. Biomaterials 2004;25:895–906.
[45] Kennedy SB, Washburn NR, Simon Jr CG, Amis EJ. Biomaterials 2006;27:3817–24.
[46] Saad B, Keiser OM, Welti M, Uhlschmid GK, Neuenschwander P, Suter UW. J Mater Sci Mater Med 1997;8:497–505.
[47] Brown XQ, Ookawa K, Wong J. Biomaterials 2005;26:3123–9.
[48] Park A, Griffith-Cima L. J Biomed Mater Res 1996;31:117–30.
[49] Salgado AJ, Wang Y, Mano JF, Reis RL. Mater Sci Forum 2006;514–516:1020–4.
[50] Simon Jr CG, Eidelman N, Kennedy SB, Sehgal A, Khatri CA, Washburn NR. Biomaterials 2005;26:6906–15.
[51] Washburn NR, Yamada KM, Simon Jr CG, Kennedy SB, Amis EJ. Biomaterials 2004;25:1215–24.
[52] Sarasua JR, Arraiza AL, Balerdi P, Maiza I. Polym Eng Sci 2005;45(5):745–53.
[53] Janmey PA, McCulloch CA. Annu Rev Biomed Eng 2007;9:1–34.